

Research on the Extrusion Process of belt with Notch Description

Qi Liu, Yuwei Wang, Wenfang Zhu, Na Zhao

Northwest Institute of Mechanical and Electrical Engineering Xianyang Shaanxi China

Abstract. The extrusion process of the belt is a process in which the belt and the inner bore of the barrel undergo complex contact and collision, and the rifling gradually penetrates the belt, so that the material of the belt continues to fail and destroy. It has high instantaneous, strong impact, high temperature, high-speed change. There is a big gap between the existing theory and the actual extrusion process, and it is urgent to carry out research work on this problem. This paper analyzes the basic characteristics of elastic and plastic deformation during the extrusion process of the belt, and establishes the Johnson-Cook constitutive model of the deformation, flow and failure process of the belt material. Explicit dynamic calculations are carried out in the process of belt extrusion, and the contact problems, deformation of the belt and material flow problems during the extrusion process of the belt are discussed in depth

1. Introduction

When the artillery automatic weapon is fired, the projectile moves along the barrel under the action of high temperature and high pressure gunpowder and gas, and interacts with the barrel. The extrusion process of the belt has an important influence on the internal ballistic of the barrel weapon. However, due to the instantaneous nature of the extrusion process, it is difficult to accurately measure it by experiments. Therefore, the friction work and the rotational energy of the projectile are often considered as secondary work in the classical internal ballistics. Taking into account the energy balance equation of internal ballistics, and ignoring the extrusion process, it is considered that the projectile starts to move when the chamber pressure reaches the starting pressure, which is quite different from the actual situation [1].

The extrusion process of the belt is actually a process of contact and collision between the belt and the inner bore of the barrel, the rifling gradually penetrates the belt, and the material of the belt continues to fail and destroy. It has the characteristics of high instantaneous, strong impact, high temperature and high-speed change. The laws of advancing resistance and deformation are very complex [2-3]. Due to many difficulties, there is still a big gap between the existing research theories and the actual extrusion process, and it is urgent to carry out research work on the extrusion process.

With the development of computer level and the development of three-dimensional simulation calculation software, the research on the extrusion process has changed from the relatively simple two-dimensional calculation in the early stage to the complex three-dimensional calculation model; from the early ideal rigid-plastic material model to the current consideration of elastic belt a complex elastic-plastic constitutive model of material damage; from the early fully Lagrange finite

element method to the current ALE adaptive technique [4]. With the development of technical means, the necessary means are provided for further research on the extremely complex mechanical process of belt extrusion. In order to deeply understand the essence of the extrusion process of the belt, it is necessary to establish a more complex mathematical model that can reflect the mechanics essence of the extrusion process to solve the highly nonlinear problem in the extrusion process. The existing large-scale finite element software and computer hardware level can already meet the needs of the extrusion process simulation research.

In this paper, relying on the National Natural Science Foundation of China project "Research on the Transient Extrusion Mechanism of Projectile Based on Different Gas Pressure Loading Rates", the method of nonlinear finite element numerical simulation is used to study the mechanical mechanism of the extrusion process of the belt, and the finite element software is used to establish the nonlinear dynamics model of the extrusion process, using the explicit numerical difference algorithm to numerically simulate the nonlinear dynamics of the extrusion process of the belt, to study the formation process of the belt groove, the extrusion movement law of the belt, and the dynamic extrusion resistance and the extrusion pressure, to study the effect of friction properties on the extrusion process of the belt. The above research can provide technical support for the design and use of projectiles and barrels, provide a necessary basis for further research on the movement of projectiles in the chamber, and provide a certain useful reference for the research on improving shooting accuracy.

2. Basic assumption

The force and deformation of the belt in the process of extrusion are very complex, and it has the characteristics of high instantaneous, strong impact, large deformation, and high-speed deformation[5]. In order to simplify the model and ignore the secondary influencing factors, the following basic assumptions are made for the process of the band being squeezed into the bore [6-7]:

- (1) The jamming process is not considered, that is, the initial position of the projectile is the contact position between the elastic belt and the initial section of the slope bore, and the initial stress and deformation of the elastic belt are ignored;
- (2) After the caliper is in place, it is considered that the belt and the inclination of the slope are closely matched, and this position is used as the beginning of the projectile extrusion process;
- (3) Ignoring the imbalance problem, it is assumed that the projectile and the barrel axis are concentric, and the friction force and motion resistance are both along the axis direction;
- (4) The influence of air resistance and shock wave at the front of the projectile is ignored;
- (5) The stress and deformation of the barrel and projectile under gravity are not considered;
- (6) The recoil movement of the body tube is not considered.

3. Model establishment

3.1 Johnson-Cook constitutive model

In the artillery structure, most structural materials adopt the elastic material constitutive relationship, and the constitutive relationship of the material in the elastic stage can be expressed as [8]:

$$\sigma = E\varepsilon \quad (1)$$

Where E is the elastic modulus.

The relationship between the stress and strain of the elastic band material, when the stress is less than the yield stress of the material, shows a linear relationship between the stress and the strain, and the deformation of the material is elastic [9]. As the material stress continues to increase beyond the yield stress, the relationship between stress and strain is no longer linear, as shown in Figure 1.

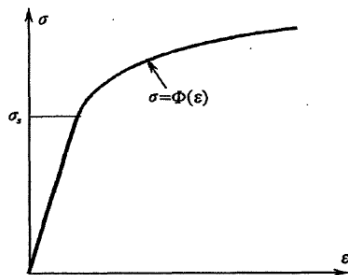


Fig. 1 Stress-strain curve of elastic band material

The elastic band not only produces plastic deformation during the extrusion process, but also is affected by the high temperature and high strain rate of the gunpowder

gas. In the finite element model established in this paper, the constitutive model used for the elastic band material is the Johnson-Cook model. The Cook constitutive model is an empirical constitutive equation. Considering the effects of temperature and strain rate, the Johnson-Cook material model consists of two parts [10-11].

Part I: The Johnson-Cook Plasticity Model

In the Johnson-Cook plasticity model, the Von Mises yield stress is a function of plastic strain, strain rate, and temperature.

$$\bar{\sigma} = (A + B \varepsilon_p^n) \left[1 + C \ln \frac{\dot{\varepsilon}^*}{\dot{\varepsilon}_0} \right] (1 - T^{*m}) \quad (2)$$

$$T^* = \frac{T - T_r}{T_m - T_r} \quad (3)$$

$$\frac{\dot{\varepsilon}^*}{\dot{\varepsilon}_0} = \frac{\dot{\varepsilon}_p}{\dot{\varepsilon}_0} \quad (4)$$

Where ε_p is the equivalent plastic strain; $\dot{\varepsilon}_p$ is the equivalent plastic strain rate; $\dot{\varepsilon}_0$ is the reference strain rate; T is the temperature; T_r is the reference temperature, generally taking room temperature; T_m is the melting temperature; A 、 B 、 C 、 m and n are constants.

The temperature change caused by the adiabatic process is:

$$\Delta T = \int_0^{\varepsilon_p} \chi \frac{\bar{\sigma} d\varepsilon_p}{\rho c_p} \quad (5)$$

In the formula, ρ is the material density; c_p is the constant volume specific heat; χ is the Taylor-Quinney coefficient, which represents the ratio of plastic work into heat, generally 0.85 to 0.95.

Part II: Johnson-Cook Fracture Failure Model

The Johnson-Cook fracture failure model defines damage in terms of the equivalent plastic failure strain [12]:

$$\varepsilon_f^{JC} = [D_1 + D_2 \exp(D_3 \sigma^*)] \left[1 + D_4 \ln \frac{\dot{\varepsilon}^*}{\dot{\varepsilon}_0} \right] (1 + D_5 T^*) \quad (6)$$

$D_1 \sim D_5$ is the material fracture failure parameter; σ^* is the stress triaxiality, that is, the ratio of the hydrostatic stress σ_m to the Von Mises equivalent stress σ_{eq} :

$$\sigma^* = \frac{\sigma_m}{\sigma_{eq}} \quad (7)$$

3.2 Explicit kinetic theory

The explicit dynamic analysis method is to use the central difference method to solve the dynamic finite element equations. The basic idea is that the acceleration is given by the first-order central difference of the velocity, and

the velocity is given by the first-order central difference of the displacement. [13]:

$$A(t_n) = \left[V\left(t_{n+\frac{1}{2}}\right) - V\left(t_{n-\frac{1}{2}}\right) \right] / \frac{\Delta t_{n-1} + \Delta t_n}{2} \quad (8)$$

$$V\left(t_{n+\frac{1}{2}}\right) = \frac{U(t_{n+1}) - U(t_n)}{\Delta t_n} \quad (9)$$

The step size of the time step and the time start and end points are defined by the following formulas.

$$\Delta t_{n-1} = t_n - t_{n-1}, \quad \Delta t_n = t_{n+1} - t_n \quad (10)$$

$$t_{n-\frac{1}{2}} = \frac{t_n + t_{n-1}}{2}, \quad t_{n+\frac{1}{2}} = \frac{t_{n+1} + t_n}{2} \quad (11)$$

The central difference method is a conditionally stable algorithm that requires relatively small time steps to maintain a stable state. Theoretically, the critical time step to maintain numerical stability should satisfy Equation [14]:

$$\Delta t_n \leq \frac{2}{\omega} \quad (12)$$

where ω is the highest order natural vibration frequency of the smallest element in the system.

4. Research on the extrusion process of a large-caliber artillery shell belt

4.1 Geometric model establishment

The extrusion process of the belt is shown in Figure 2. The projectile starts from the position of the caliper, and is pushed by the gunpowder gas acting on the bottom of the bullet to overcome the extrusion resistance and advance along the axial direction of the slope until the rear end of the elastic belt is fully squeezed into the entire belt. The rifling is deep.

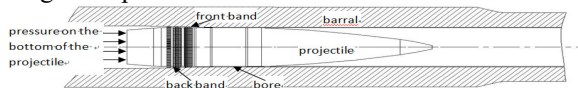


Figure 2 Schematic diagram of the extrusion process of the belt

The projectile studied in this paper consists of two elastic belts and a closed gas ring. Each of the two elastic belts has a transverse groove to accommodate the deformed material of the elastic belt. The rear elastic belt has a flange, and the rear elastic belt flange is removed from the elastic belt. The radius is large, and the rest part has a small amount of interference with the yin line of the barrel, which is conducive to the positioning of the projectile caliper. The two-dimensional cross-sectional view of the elastic belt and the closed gas ring is shown in Figure 3.



Figure 3 Two-dimensional cross-sectional view of the belt

In NX10, the geometric entity of the barrel is obtained by rotation, and the geometric entity has different tapers; in

order to simplify the calculation, the rifling angle is ignored, and the straight rifling is modeled. A section of the barrel of the bore is used as the barrel model for this calculation; the two-dimensional outline of the elastic belt is rotated circularly along the axis of the barrel to form a three-dimensional solid model of the elastic belt and the closed gas ring; Obtained by axial rotation of the axis. In this paper, a large-caliber bottom concave projectile is taken as the research object. According to the actual positional relationship between the projectile body, the elastic belt and the closed gas ring, the assembly model of the projectile body and the elastic belt is established as shown in Figure 4.

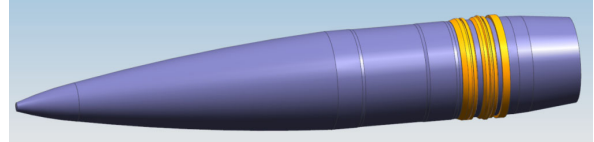
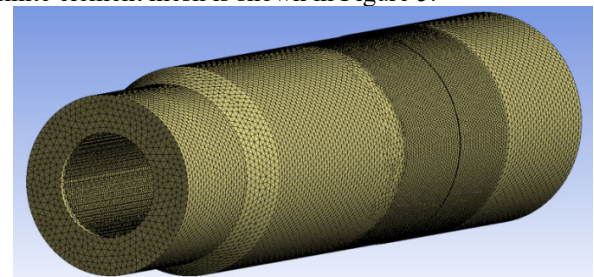


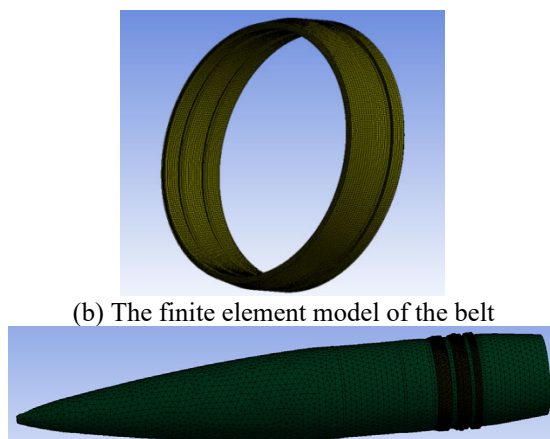
Figure 4 Assembly drawing of the belt of the projectile body

4.2 Finite Element Discrete

Save the established body tube geometry as an STP format file, and import the STP format file in the Geometry module of the WORKBENCH platform. The rifling section is meshed by using the two-dimensional meshing technique, and the two-dimensional mesh of the barrel section is swept by the three-dimensional mesh SWEEP division function, so as to obtain the three-dimensional mesh of the barrel; the contact between the elastic belt and the inner wall of the groove is obtained. Algorithm-based, secondary contact algorithm, the mesh of the secondary surface needs to be subdivided. In the contact, the surface composed of the elastic belt is selected as the secondary surface, and the elastic belt element is subdivided. The finite element size of the two elastic belts and the closed air ring is selected as 0.5mm. The element is divided, and the SWEEP method is used to sweep and divide; the finite element mesh of the projectile is also divided according to the above steps, but the projectile is a secondary consideration during the extrusion process, and the relative deformation is small, so the projectile's The finite element mesh size is large, the maximum element size is 10mm, and the final divided finite element mesh is shown in Figure 5.



(a) The finite element model of the barrel



(b) The finite element model of the belt
 (c) Finite element assembly model of missile body and belt

Fig. 5 The finite element model of the extrusion process

4.3 Material properties

Since the material of the elastic band is softer than the barrel and projectile, the material of the barrel and the projectile is considered to be alloy steel. In this simulation, the elastic-plastic constitutive model is used, and the material parameters are shown in Table 1.

Table 1 Material parameters of projectile and barrel

	density $\rho(kg/m^3)$	elastic Modulus $E(GPa)$	poisson's ratio μ	initial yield limit $\sigma_0(GPa)$	strength criterion
projectile	7820	2.03	0.3	0.980	Von-Mises
barrel	7820	2.03	0.3	1.030	Von-Mises

The elastic band material is red copper, which is widely used because of its good elasticity and plasticity and meets the requirements of the elastic band material, and the closed gas ring material is nylon material. Determining the parameters of the Johnson-Cook model of the elastic band material is very important to accurately simulate the extrusion process [6, 10]. The parameters of the elastic material constitutive model used in this paper are shown in Table 2.

Table 2 Parameters of Johnson-Cook constitutive model of copper material

Physical quantity	Parameter value	Physical quantity	Parameter value
density $\rho(kg/m^3)$	8960	shear Modulus $G(GPa)$	47.7
bulk modulus $K(GPa)$	143	specific heat CP	399

static yield stress $A(GPa)$	0.12	melting temperature $T_m(K)$	1356
hardening parameters $B(GPa)$	1.43	reference temperature $T_r(K)$	293
strain rate parameter C	0	hardening Index n	0.5
hardening Index $\dot{\epsilon}_0$	1	maximum failure plastic strain	0.5

4.4 Boundary conditions

Ignoring the self-weight of the barrel and the projectile, the six degrees of freedom of the bottom end face of the barrel are restrained, and the bottom pressure curve shown in Figure 6 is applied to the bottom of the bullet.

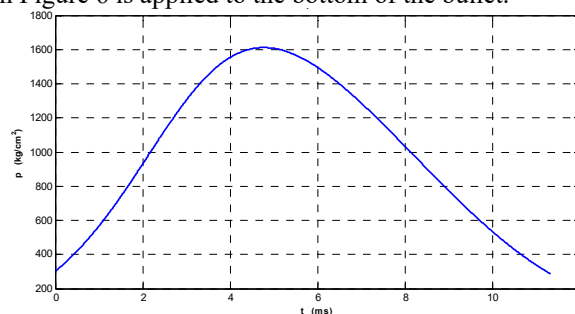


Fig. 6 Bottom pressure curve

Since the elastic belt and the projectile body belong to an interference fit, in the Explicit Dynamics module, the contact surface of the two is set to BOUNDED, the setting of the closed gas ring is consistent with the elastic belt, and the contact between the barrel or the rifling and the elastic belt adopts dynamic penalty. function method. In this paper, the relevant numerical simulation is carried out on the basis of dynamic modeling. Since the elastic-plastic constitutive, large deformation and contact problems are involved at the same time, the calculation consumes a lot of computer time. The solver used in this paper is AUTODYN, the total simulation time is 20ms, the minimum integration step is 0.01ms, the maximum integration step is 0.5ms, and the calculation results of the squeeze are saved every 1ms.

5. RESULT ANALYSIS

Figure 7 shows the resistance curve of the elastic band with the extrusion distance. It can be seen that the extrusion resistance increases continuously with the extrusion process. The maximum extrusion resistance is 83346N. At the beginning of the extrusion process, the extrusion resistance increases. Very quickly, and then it grows slowly. At the end of the squeeze, the squeeze resistance almost no longer increases, indicating that the squeeze process is completed, and the elastic bands have been embedded in the barrel rifling of the barrel. Figure 8

is the cloud diagram of the stress and deformation of the elastic belt at the beginning of the extrusion process, when the elastic belt just begins to contact the rifling. It can be seen from the figure that at this time, the maximum stress of the elastic belt is 72.5MPa, and the material of the elastic belt is still in the elastic deformation stage. The rifling stress traces can be seen from the edge, and due to the extrusion of the elastic belt by the smooth groove, the deformation of the elastic belt is mainly concentrated on the front end of the elastic belt, and the maximum deformation is 2.726mm.

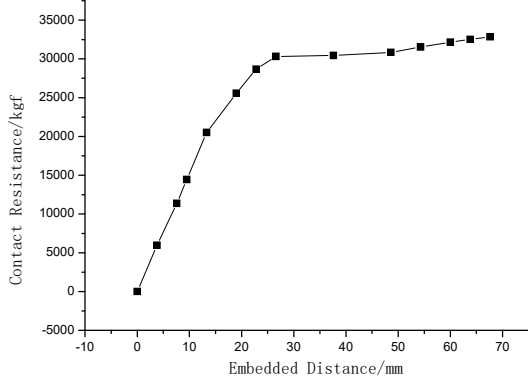


Fig.7 Variation curve of extrusion resistance with extrusion distance

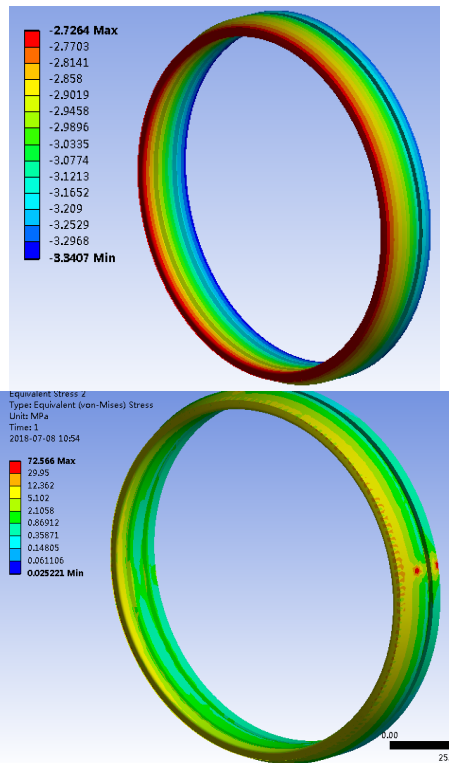


Fig.8 Cloud diagram of initial stress and deformation of front belt extrusion

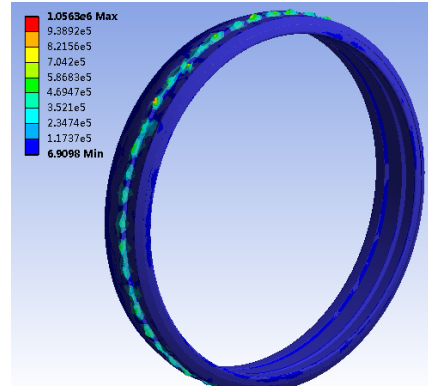
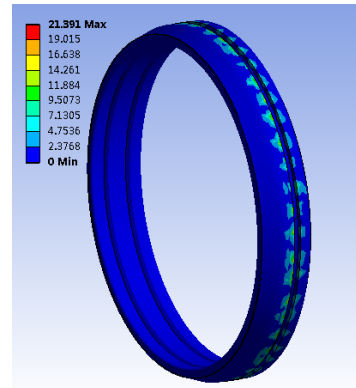


Figure 9. Cloud diagram of force and deformation after the front belt is squeezed in

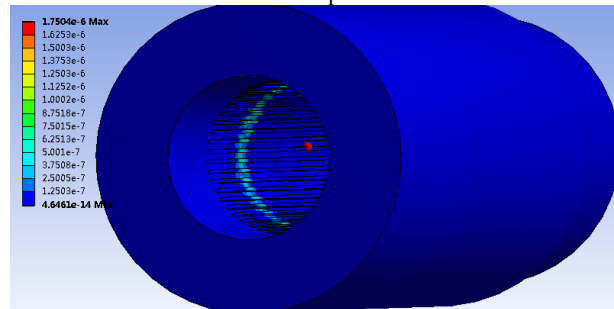


Figure 10 Force cloud diagram of the barrel during the extrusion process

Figure 9 shows the cloud diagram of the force and deformation of the elastic belt after the front elastic belt is squeezed in. It can be seen from the figure that when the front elastic belt is completely squeezed into the full rifling depth, the maximum stress of the elastic belt is 10565MPa, which exceeds the yield limit of the elastic belt material. , the elastic belt produces plastic deformation, and material flow and failure occurs at the part in contact with the rifling, resulting in a sawtooth-shaped permanent deformation similar to the shape of the rifling. It can be seen from Figure 8 that after the front elastic band is squeezed in, the maximum flow distance of the elastic band material is 21.39mm.

Figure 10 shows the force cloud diagram of the barrel after the elastic belt is completely squeezed into the rifling. It can be seen from the figure that the torus surface in contact with the elastic belt is subjected to greater force, and as the elastic belt is squeezed into the process, the force is greatly reduced. The larger force of the torus gradually moves towards the muzzle.

In order to verify the accuracy of the model, based on the test data of a simulation engraving test device to a certain caliber howitzer, the established simplified chip model was used to calculate the engraving resistance. The calculation results and test results are shown in Table 1 and Figure 2.

6. Conclusion

(1) The extrusion resistance increases continuously with the extrusion process. The maximum extrusion resistance is 83346N. In the early stage of the extrusion process, the extrusion resistance increases rapidly, and then increases slowly. At the later stage of extrusion, the extrusion resistance is almost constant. If it increases again, it shows that the entire elastic belt has completely entered the rifling of the cylindrical part of the barrel, which is in line with the physical law of the projectile extrusion process;

(2) When the elastic belt is fully squeezed into the full rifling depth, the maximum stress of the elastic belt exceeds the yield limit of the material, the elastic belt undergoes plastic deformation, and material flow and failure occur at the part in contact with the rifling, resulting in a similar shape to the rifling. The zigzag permanent deformation of the elastic band, when the extrusion is completed, the maximum flow distance of the elastic band material is about 21mm;

(3) Using the explicit dynamics method, the Johnson-Cook model is used for the elastic band material, which can not only obtain the resistance along the extrusion process, but also describe the deformation of the elastic band and the flow of the material during the extrusion process.

References

1. Jin Zhiming, Zeng Simin. Calculation and research of projectile extrusion process [J] . Journal of Ordnance Engineering, 1991.2. No.1: 7-13.
2. Xu Shaojie, Chen Xiong, Feng Xiaobing. Numerical simulation and analysis of a certain type of artillery shell belt extrusion [J] . Sichuan Ordnance Science, 2011.32. No.8: 14-15.
3. Wang Peng, Yang Guolai, Ge Jianjian, etc. Numerical simulation of elastic belt extrusion process based on Johnson-Cook constitutive model [J] . Chinese Journal of Ballistics, 2015.27. No.2: 55-56.
4. Sun Quanzhao, Yang Guolai, Wang Peng, etc. Numerical simulation research on the extrusion process of a large-caliber howitzer shell belt [J] . Journal of Ordnance Engineering, 2015.36. No.2: 206-207.
5. Li Miao, Qian Linfang, Chen Longmiao. Research on the internal ballistic characteristics of the elastic belt extrusion process [J] . Vibration and Shock, 2016, 35(23): 78-79.
6. Liu Chengzhu. Study on the structural parameters of large-caliber artillery that affect the initial disturbance of the projectile[D]. Nanjing: Nanjing University of Science and Technology, 2016: 8-11.
7. Jin Zhiming, Zeng Simin. Calculation and research of projectile extrusion process[J] . Journal of Ordnance Engineering, 1991 (1): 7-13.
8. Chen, Peter C. Analysis of Engraving and Wear in a Projectiler Rotating Band[R]. 1999.
9. South Joseph, Yioumas Aristedes, A Study of the Engraving of the M855 5.56mm Projectile [R]. 2008.
10. Lin Gui. Design of the simulation experiment device for the high-speed extrusion of the elastic belt into the rifling process [D]. Nanjing: Nanjing University of Science and Technology, 2014: 31-35.
11. Gu Wei. Numerical simulation research on belt extrusion and gun bore damage [D] . Nanjing: Nanjing University of Aeronautics and Astronautics, 2014: 27-32.
12. Jiang Zeyi. Research on projectile extrusion process [D] . Taiyuan: North Central University, 2014: 28-29.
13. Zhang Zhihong. Research on wear behavior of barrel coating based on ABAQUS [D] . Lanzhou: Lanzhou University of Technology, 2016: 7-10.
14. Zhang Hao, Zhou Yanhuang. Research on the extrusion process of submerged artillery [J]. Chinese Journal of Ballistics, 2006, 18(1): 76-77.